Hydrol. Earth Syst. Sci. Discuss., 9, 3237–3267, 2012
www.hydrol-earth-syst-sci-discuss.net/9/3237/2012/
doi:10.5194/hessd-9-3237-2012

Hydrology and Earth System Sciences Discussions

A conceptual remote sensing based interception-infiltration model for regional and global applications

M. Tum[1] **and E. Borg**[2]

[1]Deutsches Zentrum für Luft- und Raumfahrt (DLR), Deutsches Fernerkundungsdatenzentrum (DFD), Oberpfaffenhofen, 82234 Wessling, Germany
[2]Deutsches Zentrum für Luft- und Raumfahrt (DLR), Deutsches Fernerkundungsdatenzentrum (DFD), Kalkhorstweg 53, 17235 Neustrelitz, Germany

Received: 23 February 2012 – Accepted: 6 March 2012 – Published: 12 March 2012

Correspondence to: M. Tum (markus.tum@dlr.de)

Published by Copernicus Publications on behalf of the European Geosciences Union.

Abstract

We present a remote sensing driven modelling approach to simulate the one dimensional water transport in the vadose zone of unsaturated soils on a daily basis, which can be used for regional to global applications. Our model needs van Genuchten parameters to calculate the hydraulic conductivity, which we estimated using the ISRIC-WISE Harmonized Global Soil Profile Dataset Ver. 3.1 and the Rosetta programme. We calculated all needed parameters for 26 global main soil types and 102 soils of second order, which are based on the original, global FAO 1974 soil classification. Soil depth and the layering of one to six layers were defined for each soil. The parameters for the main soils are presented in this paper. Interception by vegetation is also considered using remote sensing calculated Leaf Area Index (LAI) time series from SPOT-VEGETATION. Precipitation is based on daily time series from the European Centre for Medium-Range Weather Forecasts (ECMWF). For Germany we compared our model output with soil moisture data from the ECMWF, which is based on the same precipitation dataset. We found a good agreement for the general characteristics of our modelled plant available soil water with this dataset, especially for soils which are close to the standard characteristics of the ECMWF. Disagreements were found for soils under stagnant moisture and for shallow soils, which are not considered in the ECMWF model scheme, but can be distinguished with our approach. The proposed approach for combining established model formulations for interception and one-dimensional vertical water transport with time-series of remote sensing data intends to contribute to the realistic parameterization of the soil water budged. This is especially needed for the global and regional assessment of e.g. net primary productivity which can be calculated with vegetation models.

HESSD

9, 3237–3267, 2012

1 Introduction

The prediction of hydrodynamics in unsaturated soils remains a challenging task in the topic of soil physics and is important for modelling physical processes which are related to the soil water content. During the last years the development of models capable to simulate the water flow in soils has gained an important role. In this context, computer models based on the numerical solution of Richards' equation has proved as being valuable. Their application is often restricted by a lack of hydraulic property information involving the soil water retention curve (SWRC) and the unsaturated hydraulic conductivity. For modelling the SWRC many diverse empirical approaches can be found (e.g. Gardner, 1958; Brooks and Corey, 1964; Campbell, 1974; van Genuchten, 1980; Hutson and Cass, 1987; Russo, 1988). Usually many input parameters are required to describe the soil processes. Due to inherent temporal and spatial variability of hydraulic properties in nature, large numbers of samples are generally required to properly characterize the spatial distribution of these hydraulic properties. Therefore, direct measurements are time-consuming and expensive. In contrast, indirect methods are increasingly used to provide estimates. Presuming Richards' equation can be applied, the most crucial point is the exact measurement and description of hydraulic properties, or to be more precise: the soil water retention curve $\theta(h)$ and the hydraulic conductivity function $k(\theta)$, where θ is the volumetric water content, h the pressure head and k the hydraulic conductivity. To solve this problem diverse pedotransfer functions (PTFs) have been developed (e.g. Vereecken et al., 1989; Wosten, 1997; Mayer and Jarvis, 1999; Minasny and McBratney, 2000; Schapp et al., 2001; Jarvis et al., 2002; Tomasella et al., 2003; Weynants et al., 2009; Wessolek et al., 2011). A comprehensive overview of developed pedotranfer functions in soil hydrology can be found in Pachepsky and Rawls (2005), allowing a good understanding of state-of-the-art modelling approaches with respect to advantages and restrictions of pedotransfer functions to predict hydrological soil properties.

HESSD
9, 3237–3267, 2012

To couple these complex physics of water transport in soil with the atmosphere and vegetation an interception model has to be considered. The capacity of vegetation to intercept water is of great importance, since the rate of evaporation from wet canopy is higher than from dry canopy conditions (Stewart, 1977). Thus rainfall interception and its following rainfall evaporation may result in a net loss to the system, but depending on the surrounding conditions (e.g. coastal or mountain fog belts), could also lead to a net gain (Bruijnzeel, 2000). As a consequence the presence or absence of vegetation strongly affects the amount of rainfall reaching the soil surface. Model formulations to describe interception of vegetation have been developed (e.g. Rutter et al., 1971; Gash, 1979; Massman, 1983; Xiao et al., 2000) which use parameters to describe the threshold amount of rain that can be stores in the canopy and a descriptive parameter for the canopy structure. The Braden (1985) and Calder (1986) models are further examples which use information of Leaf Area Index (LAI) to describe the canopy instead of a descriptive parameter. A review about approaches to model interception was recently published by Muzylo et al. (2009).

The second interaction of vegetation with soil water, namely water suction via roots and its following evapotranspiration by vegetation is a further influencing factor to the available soil water content. However in this study we will not focus on the description of this process.

The primary objective of this study is to introduce our soil water transport model, which is suitable to calculate the soil water balance on a regional to global scale. It is driven by van Genuchten parameters and remote sensing data and distinguishes 128 soils, which follow the system of the original FAO-UNESCO legend (FAO-UNESCO, 1974). We compared our model results with modelled time series taken from the European Center for Medium Range Weather Forecast (ECMWF), which are based on the same precipitation dataset we used. With our approach to combine established model formulations with the use of remote sensing data, we see the potential in our model to be applied in remote sensing based vegetation models. In vegetation models the realistic parameterisation of the soil water budged is a challenging task, but

HESSD
9, 3237–3267, 2012

of major interest, since it is usually very simplified.

2 Theoretical background

In our model the water balance is considered regarding the two reservoirs which influence the water availability and is affected by vegetation: soil water and intercepted water on leaves and other parts of vegetation. These reservoirs change in time and space depending on precipitation, temperature and evapotranspiration. Evaporation from soil is calculated daily following the approach of Ritchie (1972). Transpiration is not considered in our model formulation.

The processes of interception and percolation, on which we focused on in this study will be discussed in more detail in the next sections.

2.1 Interception

Interception (P_i) is considered following the concept of Braden (1995). The general assumption of this approach is that P_i is empirically related to the Leaf Area Index (LAI, Λ), the fraction of canopy closure (f_c) and the precipitation sum (P):

$$P_i = f_c \left[1 - \left(1 + b_0 \left(P - P_{sn}\right)/f_c\right)^{-1}\right] \quad (1)$$

where b_0 is the fraction of soil covered by plants and P_{sn} the share of precipitation which reaches the ground as snow, which is not considered as available for soil infiltration. Snowfall is calculated as linear function according to Wigmosta et al. (1994), falling linearly from P to 0 between $-1.1\,^{\circ}$C and $3.3\,^{\circ}$C. Since b_0 and f_c are both related to Λ one might express b_0 and f_c following Eqs. (2) and (3):

$$b_0 = 1 - \exp\left(-0.5\,\Lambda\right) \quad (2)$$

$$f_c = \frac{\Lambda}{\Lambda_{lim}\, f_{c\,max}} \quad (3)$$

HESSD
9, 3237–3267, 2012

where Λ_{lim} is the limiting LAI, which is set to 3 assuming LAIs greater than 3 do not influence the canopy fraction by raising it. $f_{\text{c max}}$ represents the maximum share of canopy fraction and is set to 0.9, assuming the maximum fraction of cover per grid cell cannot be higher than 90 %.

Evaporation from canopy is calculated taking into account both: the dropping loss of water from leafs (P_{d}) the disposition of water in the skin reservoir (W_{s}), but is limited by the evaporation from canopy (E_{c}):

$$P_{\text{d}} = W_{\text{s}} + P_{\text{i}} - 0.1\,\Lambda - E_{\text{c}} \text{ with } P_{\text{d}} \geq 0. \tag{4}$$

E_{c} is calculated following the scheme of Philip (1957), assuming limitation at the maximum potential evaporation rate (E_{cpot}):

$$E_{\text{c}} = \begin{cases} P_{\text{i}} - P_{\text{d}} + W_{\text{s}} & \text{with } E_{\text{c}} < E_{\text{cpot}} \\ E_{\text{cpot}} & \text{with } E_{\text{c}} \geq E_{\text{cpot}} \end{cases}. \tag{5}$$

The skin reservoir is considered as a cumulative reservoir which is filled and drained over time by precipitation, throughfall and evaporation from the canopy. We assume the skin reservoir to be empty at time step $j = 0$:

$$W_{\text{s}}^{j} = \begin{cases} W_{\text{s}}^{j-1} + P_{\text{i}} - P_{\text{d}} - E_{\text{c}} & \text{with } W_{\text{s}}^{j} < f_{\text{c}} \\ f_{\text{c}} & \text{with } W_{\text{s}}^{j} \geq f_{\text{c}} \end{cases} \text{ and } j \geq 1. \tag{6}$$

Finally the ground reaching precipitation without being interfered by vegetation i.e. throughfall (P_{t}) can be expressed as:

$$P_{\text{t}} = \begin{cases} P_{\text{d}} + P - P_{\text{i}} & \text{with } W_{\text{s}} < f_{\text{c}} \\ P_{\text{d}} + P - P_{\text{i}} + \left(W_{\text{s}}^{j-1} + P_{\text{i}} - P_{\text{d}} - E_{\text{c}} - f_{\text{c}}\right) & \text{with } W_{\text{s}} = f_{\text{c}} \end{cases}. \tag{7}$$

2.2 Infiltration

The process of water, penetrating the soil surface is defined as infiltration. It has a dominant role among the components of hydrological processes of catchment areas

HESSD
9, 3237–3267, 2012

(Dyck, 1980). We base our approach on an adaption of the one-dimensional vertical transport algorithm described by Syring and Kersebaum (1989), which is based on the theoretical approach of Dyck (1980) and Anlauf et al. (1989). The vertical transport within the soil is calculated using a combination of the Darcy-equation (Eq. 8) with the local balance (or continuity) equation (Eq. 9).

$$q_w = -k\left(\frac{d\psi}{dz} - 1\right) \tag{8}$$

$$\frac{\partial\theta}{\partial t} = -\frac{\partial q}{\partial z} + A(t, z) \tag{9}$$

Here q_w represents the water flux from a layer to its subjacent layer. k is the hydraulic conductivity of the soil water flux, which is dependent on the matric potential ψ and the depth of layer z. The local balance equation describes the relation of time (t) dependent volumetric soil water content (θ) and soil layer depth depending water flux. Parameter A represents the source or sink term as function of depth and time.

When combining Eqs. (8) and (9) the problem can be described by Richard's-equation:

$$\frac{\partial\theta}{\partial t} = -\frac{\partial\left[k\left(\frac{\partial\psi}{\partial z} - 1\right)\right]}{\partial z} + A(t, z). \tag{10}$$

The matric potential depending on volumetric soil water content (θ_ψ) and hydraulic conductivity (k_ψ) can be calculated following the approach proposed by van Genuchten (1980):

$$\theta_\psi = \theta_r + (\theta_s - \theta_r)\left[1 + \left(\alpha|\psi|\right)^n\right]^{\left(1-\frac{1}{n}\right)} \tag{11}$$

HESSD
9, 3237–3267, 2012

$$k_\psi = k_s \frac{\left(1 - (\alpha|\psi|)^{n-1}\left(1 + (\alpha|\psi|)^n\right)^{\left(1-\frac{1}{n}\right)}\right)^2}{\left(1 + \left((\alpha|\psi|)^n\right)^{\frac{\left(1-\frac{1}{n}\right)}{2}}\right)} \quad (12)$$

where θ_r is the volumetric soil water content at the permanent wilting point (PWP), θ_s the volumetric soil water content and k the hydraulic conductivity at saturation. The parameters $\alpha$and n represent two form parameters which are needed for the van Genuchten approach. Since α, n, k_s, θ_r and θ_s are highly empirically derived, it is discussed as challenging to derive van Genuchten parameters on a broader scale (Schaap et al., 2001). We used soil profiles and the Rosetta programme to define these parameters, which will be discussed later in more detail. Because θ_ψ and k_ψ are functions of the matrix potential ψ Eq. (10) can be used to determine ψ. Equation (10) itself is a differential equation of second order.

In a first step the starting conditions of the upper and lower boundary have to be defined. At its upper boundary the whole amount of throughfall can infiltrate until the soil dependent saturated condition is reached. The top layer of each soil type is set to 3 cm, since it is assumed that only the upper 3 cm can directly react to precipitation and thus evaporate water. At saturation ψ is set to 0:

$$z = 0, t > 0 : P_t = k\left(\frac{\partial\psi}{\partial z} - 1\right) \text{ and } \psi \leq 0. \quad (13)$$

At the lower boundary (ψ_L), ψ is set to zero in the case that a soil under stagnant moisture condition as for instance gleyic soils is modelled. Otherwise ψ_L is set to −15 000 to simulate a soil layer with dry conditions and to respect water run off processes, or to be more precise: to allow water to leave the system.

HESSD
9, 3237–3267, 2012

In a second step for all layers (i) between the upper and lower boundary, with the specific thickness Δz, the water flux between two soil layers q_i is calculated:

$$q_i = k_{i+0.5} \left\{ \frac{(\psi_{i+1} - \psi_i)}{\Delta z} - 1 \right\}. \quad (14)$$

To calculate the hydraulic conductivity of the inner compartments we followed the approach of Syring and Kersebaum (1988) who used the arithmetic average of the two surrounded compartments:

$$k_{i+0.5} = 0.5 \, [k(\psi_i) + k(\psi_{i+1})]. \quad (15)$$

Thus for each inner layer i at time step t, ψ can be expressed as:

$$\psi_t = \psi_{t-1} - 0.5 \, \Delta z \left(1 - \frac{q_i}{k_{0.5}} \right) \text{ with } \psi_t \leq 0. \quad (16)$$

To solve this equation a variation of the Newton-algorithm (Remson et al., 1971) was considered to calculate the function f of ψ:

$$f(\psi_i) = \frac{\left(\theta_i^j - \theta_i^{j-1}\right)}{\Delta t} + \frac{\left(\theta_i^j - \theta_{i-1}^j\right)}{\Delta z} - A_{t,z}. \quad (17)$$

Following this one may approximate ψ as:

$$\psi_i^* \approx \psi_i - \frac{f(\psi_i)}{\left(\frac{\partial f(\psi_i)}{f \; \psi_i}\right)}. \quad (18)$$

3 Input data

3.1 Van Genuchten parameter

For our modelling approach we used, as described above, van Genuchten parameters, which were estimated by using the Rosetta program (Schaap et al., 2001). Rosetta

HESSD
9, 3237–3267, 2012

contains a neuronal network to predict van Genuchten parameters which are based on estimates on grain size distribution (sand, silt and clay content) of a soil. The original FAO legend distinguishes 26 main soil types and 102 soils of second order. In order to estimate the mean grain size distributions for the 128 FAO soils we used the ISRIC-WISE Harmonized Global Soil Profile Dataset Ver. 3.1 (Batjes, 2009), which contains data of 10,253 soil profiles and is classified following the system of original and revised FAO-UNESCO legends (FAO-UNESCO, 1974; FAO, 1980).

Since for the reported soils individual measurements had wide ranges of total layers (2–12 layers) we decided to calculate – in a first step – the median of reported soil layers for each soil type. This was done to minimize the complexity of soils and to minimize the computational effort. In a second step we calculated the average grain size distribution and layer depth for the soil profiles which were selected in the first step. Other reported soil profiles with more or less layers than the median were not used for the calculation. For the main soils these values and the correspondent van Genuchten parameters are presented in Table 1.

To obtain spatial information for the global soil type distribution we used the Harmonized World Soil Database (HWSD) provided by the International Institute for Applied Systems Analysis (IIASA). The HWSD is freely available as grid with 30˚ arc seconds resolution in a latitude-longitude projection using the WGS84 (World Geodetic System 1984) datum (FAO/IIASA, 2009). It contains information about the dominant soil type, following the systems of the FAO from 1974, 1985 and 1990, depending on the location on earth.

Since we estimated our van Genuchten parameters for the FAO '74 soil classification we harmonized the HWSD dataset to this classification scheme, by transforming newer classifications to the 74' standard.

3.2 Remote sensing data

For our modeling approach we used LAI time-series of 10-days data-composites derived using satellite remote sensing data. The LAI describes the phenology of

HESSD
9, 3237–3267, 2012

vegetation and thus controls interception. We used LAI time series based on CYCLOPES which can be downloaded from the POSTEL (Pole d'Observation des Surfaces continentales par Teledetection) database. This global dataset is freely available for the period 1999–2007 with a spatial 1 km^2 resolution. Since the HWSD soil map is also available on this resolution no spatial interpolation is needed to be applied. However, for each pixel analysis of the LAI time series was conducted to fill data gaps and eliminate outliers, using harmonic analysis (HA), which is based on Bittner (1993). This was needed since our model needs gap-free and continuous time series. HA decomposes a time series into a linear combination of suitable trigonometric functions, i.e. sine and cosine oscillations of particular periodicities. The HA technique corresponds to an approximate deconvolution of the power spectrum by iteratively finding and subtracting the highest peak of the time series power spectrum. This method was adapted for the correction of LAI time series data (Niklaus et al., 2012).

4 Results and discussion

For a regional quality assessment we chose to compare our model results with data taken from the ECMWF ERA-INTERIM re-analysis. The spatial resolution of this dataset is 0.25° × 0.25°. The temporal resolution is a daily time step. Since this dataset is based on the same precipitation dataset we presuppose in a general comparability of the two products. We chose the time period of 2002 to 2007 as observation time and the German territory as simulation area. The November and December 2007 were excluded from the analysis due to massive changes in the ECMWF model approach. The ECMWF numerical weather model subdivides a 289 cm soil core into 4 layers (7 cm, 21 cm, 72 cm and 189 cm), with PWP at 0.171 % and field capacity (FC) at 0.323 % water content, which is assumed to be valid global. Infiltration obeys the Darcy Law and is effected by evaporation from the bare soil portion and evapotranspiration from vegetation.

HESSD
9, 3237–3267, 2012

Our model – in contrast – treats each soil type depending on its calculated grain size distribution and layering. In Fig. 1 the distribution of the eleven main FAO soil types for Germany is presented.

From Fig. 1 it is apparent that Germany's soil cover can be characterized using eleven soil types, from which Cambisols and Luvisols can be identified as dominating. However, the spatial distribution is not homogenous. The Northern and Eastern regions of Germany show the highest heterogeneity of soil cover, whereas the middle regions of Germany are more homogeneous and dominated by Cambisols and Luvisols. Mountain ranges as the northern Alps, the "Fraenkische Alp" are covered with Lithosols, a very shallow soil which we assume to have only 10 cm depth.

In order to compare the soil water characteristics we calculated the mean plant available soil water content for the observation time, for both: the ECMWF soil water content product and our own model results (Fig. 2). Analysis revealed a mean plant available soil water content for ECMWF is 364 (±59) mm. For our own estimates we found a corresponding value of 170 (±83) mm, which is roughly half of the ECMWF, but combined with a higher standard deviation. The lower water content might be explained with the fact that our soil depth ranges soil dependent from 10 cm to 208 cm, but the ECMWF soil is set static to 289 cm. Since the ECMWF data does not show rough transitions, the higher standard deviation can be explained with the fact that we take into account individual soil characteristics, based on the soil distribution as shown in Fig. 1. Considering the costal zone of the ECMWF result it becomes apparent that the lowest values can be found here. In addition for some areas no data are available, which is due to the global modeling scheme, in which costal zones are sometimes treated as water, although more than 50 % of the grid cell is covered with land, and vise versa.

To compare the ECMWF soil water product with our own estimates we calculated the root mean square error (RMSE) based on daily values for the whole observation period and area. The result is presented in Fig. 3.

HESSD
9, 3237–3267, 2012

Areas which are symbolized with blue and yellow colours indicate a good agreement of the model behaviour, whereas red colours represent areas of highly different conformability. From Fig. 3 it can be deduced that the lowest RMSEs, and thus the highest degree of agreement, can be found for regions of homogenous soils as e.g. the Cambisol-region in central Germany. The highest RMSE up to 200 can mainly be found for areas which correspond to soils under constant wet conditions, as for instance Gleysols and Fluvisols, and with regions of shallow soils (Lithosols) are reported (see Fig. 1). This is again due to higher detailed soil map which we used and our approach to respect the individual characteristics of soils (see Table 1). Therefore, our model can represent regional conditions in more detail.

When zooming to the "Oderbruch-region" located at the North-Eastern boarder of Germany this finding can be confirmed (Fig. 4). Here it can be seen that the pixels which are described as Fluvisols and Gleysols show the highest level of disagreement (red). The soil parameters for these heavy soils, also called "minute soils", are highly discrepant to the ECMWF soil properties. Areas with Arenosols, Podzols, and Podzoluvisols show intermediate (yellow) and Cambisols the best agreement (blue). This can be explained with the spatial resolution ($0.25^{\circ} \times 0.25^{\circ}$) of the ECMWF soil water content product. Heterogeneous soil landscapes, as situated here cannot be represented with this coarse resolution. Therefore, the ECMWF product has to be seen as integrative, since these differences in hydrological behaviour and soil properties are not represented.

In order to compare the inter-annual behaviour of the infiltration process of the two models we focused on three soil examples. Since the ECMWF soil bulk and compartments are not directly comparable to our individually calculated soil characteristics, but are based on the same precipitation dataset, we chose to compare the general behaviour for three soil examples (Cambisol, Gleysol, and Lithosol). The results are presented in the Figs. 5–7. The examples were chosen due to their importance to the global and European soil distribution and because of our finding of high and low agreement, as discussed above. According to the HSWD map around 9 % of global

HESSD
9, 3237–3267, 2012

soils are Cambisols and 15 % are under saturated conditions and 12 % are Lithosols. The ECMWF data was taken for latitude: 51.0°/longitude: 8.0° (Cambisol), latitude: 52.8°/longitude: 13.0° (Gleysol) and latitude: 47.6°/ longitude: 11.3° (Lithosol).

From Figs. 5 and 6 it is apparent that the volumetric water content of the two topmost layers of both models are comparable in their general characteristics, but with differences in their absolute values.

The first layer of both models is highly influenced by precipitation, which can explain the high short time variability of water content. This is to some extend also valid for the second layer, which is still highly influenced by daily precipitation events, but already shows little hysteresis effects. ECMWF third layer still shows characteristics which are highly dependent on precipitation, which was not expected, since this layer already represents the soil water content in 28 cm to 100 cm depth. Since we cannot find this behaviour in our soil layers 3 to *n* this layer cannot be compared with our model results. Our third and ECMWF forth layer can again directly be compared and show hysteresis effects and the start of long term water movement behaviour in soil.

A closer view to Fig. 5 shows a decrease in our volumetric water content from layer 1 to 6. This is due to our model formulation in which we assume a complete dry layer beneath our last model layer, to respect water run off processes, or to be more precise to allow water to leave the system. On the other hand, as can be seen from Table 1, Cambisol has low k_s values for all layers and thus a strong water holding capacity, which results in not too steep negative slopes during summer periods (e.g. 2003 and 2006). To model saturated conditions, as necessary for Gleysols, we assume a saturated layer beneath the last model layer. With this more or less steady state conditions can be achieved, as can be seen in layer 5 of Fig. 6.

In contrast Fig. 7 shows that the soil water availability of the two modelled layers of Lithosols cannot be compared with the characteristics of the corresponding ECMWF plot. Since for Lithosols we assume a soil depth of only 10 cm they are highly dependent on precipitation events and loose water immediately under non precipitation conditions. However, due to the mathematical limitations of our model, a total loss of

HESSD
9, 3237–3267, 2012

soil water cannot be modelled. A residue of minimum 3 % water always remains in the soil core.

Generally, long term water characteristics as we can describe with soil layer four to six, saturation conditions or strong water holding capacities cannot be found in the ECMWF model results. This can be expected since this additional information is not taken into account in the ECMWF model.

5 Conclusions

We adapted, refined and presented a one-dimensional soil water transport model for regional and global environmental applications, following the van Genuchten approach. It uses remote sensing based time series of the Leaf Area Index to treat interception. In addition we calculated for all 128 FAO '74 soil types the individual soil depth, layering, grain size distribution and van Genuchten parameters. In order to compare our model with other data, we applied our model for the period 2002 to October 2007 for Germany and compared the results with ECMWF soil water content data for the same period.

We found good agreements for regions of Cambisols and bad agreements for regions of soils under stagnant moisture (e.g. Gleysols) shallow soils (Lithosols) or regions of heterogeneous soil landscapes of strongly varying soil qualities at small-scale. Reasons for different agreement levels can be seen in the more detailed soil map, which was used in our adapted and refined modelling approach and in the fact that the ECMWF model only comprises one globally generalized soil type.

Modelled characteristics of the plant available soil water in the unsaturated zone are typically used for vegetation models. Therefore, our presented modelling approach could be helpful in the assessment of the soil water at a broader spatial scale. Our model will, additionally, allow assessing the soil water in vegetation models on a global, regional and local scale, if all needed data are available. However, for local applications our approach should be further tested in additional countries and for specific small scale case studies as e.g. lysimeter stations.

HESSD
9, 3237–3267, 2012

Furthermore, this new modelling approach could be seen as useful for applications which calculate the plant available soil water content in scenario models. In particular, more reliable forecasts will be of great consequence for the estimation of the impacts of global climate change upon vegetation species distributions, water availability and thus food security.

Acknowledgements. This study was conducted under the FP7 projects EnerGEO (Grant agreement no.: 226364) and ENDORSE (grant agreement no.: 262892). We thank ECMWF, ISRIC, IIASA, and MediasFrance for providing data. The authors are grateful to the anonymous reviewers.

References

Anlauf, R. K, Kersebaum, C., Ping, L. Y., Nuske-Schüler, A., Richter, J., Springob, G., Syring, K. M., and Uterman, J.: Modelle für Prozesse im Boden – Programme und Übungen, Ferdinand Enke Verlag, Stuttgart, 1987.

Batjes, N. H.: Harmonized soil profile data for applications at global and continental scales: updates to the WISE database, Soil Use Manage., 25, 124–127, 2009.

Bittner, M.: Langperiodische Temperaturoszillationen in der unteren und mittleren Atmosphäre (0 bis 100 km) während der DYNA-Kampagne, PhD. Thesis, Bergische Universität; Gesamthochschule Wuppertal, Fachbereich 8, Physik, 1993.

Braden, H.: Ein Energiehaushalts- und Verdunstungsmodell für Wasser- und Stoffhaushaltsuntersuchungen landwirtschaftlich genutzter Einzugsgebiete, Mitt. Dtsch. Bodenkdl. Ges., 22, 294–299, 1985.

Braden, H.: The Model AMBETI: A detailed description of a soil-plant-atmosphere model, Ber. Dtsch. Wetterd., 195, Offenbach am Main, Germany, 1995.

Brooks, R. H. and Corey, A. T.: Hydraulic Properties of Porous Media. Hydrology Paper No. 3, Colorado State University, Fort Collins, CO, 1964.

Bruijnzeel, L. A.: Hydrology of moist tropical forests and effects of conversion, A state-of-knowledge review, UNESCO International Hydrological Programme, Paris, 1990.

Calder, I.: A stochastic model of rainfall interception, J. Hydrol., 89, 65–71, 1986.

HESSD

9, 3237–3267, 2012

Campbell, G. S.: A simple method for determining unsaturated hydraulic conductivity from moisture retention data, Soil Sci., 117, 311–314, 1974.
Dyck, S., Becker, A., Flemming, G., Glugla, G., Golf, W., Grünewald, U., Gurtz, J., Kluge, C. and Peschke, G.: Angewandte Hydrologie, Teil 1: Berechnung und Regelung des Durchflusses der Flüsse, Teil 2: Der Wasserhaushalt der Flußgebiete, Verlag für Bauwesen, Berlin, 1980.
FAO: FAO-UNESCO Soil map of the world, revised legend, with corrections and updates, World Soil Resources Report 60, FAO, Rome, 1988.
FAO-UNESCO: Soil map of the world, 1:5,000,000, Vol. 1 – Legend, United Nations Educational, Scientific and Cultural Organization, Paris, 1997.
FAO/IIASA/ISRIC/ISSCAS/JRC. Harmonized Soil Database (version 1.1), FAO, Rome, Italy and IIASA, Laxenburg, Austria, 2009.
Gardner, W. R.: Some steady-state solutions of the unsaturated moisture flow equation with application to evaporation from a water table, Soil Sci., 85, 228–232,1958.
Gash, J. H. C.: An analytical model of rainfall interception by forest, Q. J. Roy. Meteorol. Soc., 105, 43–55, 1979.
Hutson, J. L. and Cass, A.: A retentivity function for use in soil-water simulation models, J. Soil Sci., 38, 105–113, 1987.
Jarvis, N. J., Zavattaro, L., Rajkai, K., Reynolds, W. D., Olsen, P.-A., McGechan, M., Mecke, M., Mohanty, B., Leeds-Harison, P. B., and Jacques, D.: Indirect estimation of near-saturated hydraulic conductivity from readily available soil information, Geoderma, 108, 1–17, 2000.
Knorr, W. and Heimann, M.: Uncertainties in global terrestrial biosphere modeling 1. A comprehensive sensitivity analysis with a new photosynthesis and energy balance scheme, Global Biogeochem. Cy., 15, 207–225, 2001.
Massman, W.: The derivation and validation of a new model for the interception of rainfall by forest, Agr. Meteorol., 28, 261–286, 1983.
Mayer, T. and Jarvis, N. J.: Pedotransfer functions to estimate soil water retention parameters for modified Brooks-Corey type model, Geoderma, 91, 1–9, 1999.
Minasny, B. and McBratney, A. B.: Hydraulic conductivity pedotransfer functions for Australian soil, Aust. J. Soil Res., 38, 905–926, 2000.
Muzylo, A., Llorens, P., Valente, F., Keizer, J. J., Domingo, F., and Gash, J. H. C.: A review of rainfall interception modelling, J. Hydrol., 370, 191–206, 2009.
Niklaus, M., Günther, K. P., Tum, M., and Bittner, M.: Generation of a global, gap-free SPOT-VGT LAI dataset using spectral analysis techniques, Int. J. Remote Sens., in review, 2012.

HESSD
9, 3237–3267, 2012

Pachepsky, Y. A. and Rawls, W. J.: Development of Pedotransfer Functions in Soil Hydrology, Elsevier Science, Amsterdam, 2005.
Philip, J. R.: Evaporation, and moisture and heat fields in the soil, J. Meteorol., 14, 139–158, 1957.
Remson, I., Hornberger, G. M., and Molz, F. J.: Numerical methods in subsurface hydrology, Wiley, New York, 1971.
Ritchie, J. T.: Model for predicting evaporation from a row crop with incomplete cover, Water Resour. Res., 8, 1204–1213, 1972.
Russo, D.: Determining soil hydraulic properties by parameter estimation: On the selection of a model for the hydraulic properties, Water Resour. Res., 24, 453–459, 1988.
Rutter, A., Kershaw, K., Robins, P., and Morton, A.: A predictive model of rainfall interception in forest, I. Derivation of the model from observation in a plantation of Corsican pine, Agr. Meteorol., 9, 367–384, 1971.
Schaap, M. G., Leij, F. J., and van Genuchten, M. T.: Rosetta: a computer program for estimating soil hydraulic parameters with hierarchical pedotransfer functions, J. Hydrol., 251, 163–176, 2001.
Stewart, J. B.: Evaporation from the wet canopy of a pine forest, Water Resour. Res., 13, 915–921, 1977.
Syring, K. M. and Kersebaum, K. C.: Simulation des 1-dimensionalen Wassertransportes, in: Modelle für Prozesse im Boden, edited by: Richter, J., Enke, Stuttgart, 32–49, 1988.
Tomasella, J., Pachepsky, Y., Crestana, S., and Rawls, W. J.: Comparison of two techniques to develop pedotransfer functions for water retention, Soil Sci. Soc. Am. J., 67, 1085–1095, 2003.
Van Genuchten, M. T.: A Closed-form Equation for Predicting the Hydraulic Conductivity of Unsaturated Soils, Soil Sci. Soc. Am. J., 44, 892–898, 1980.
Vereecken, H., Maes, J., Feyen, J., and Darius, P.: Estimating the soil moisture retention characteristics from texture, bulk density and carbon content, Soil Sci. Soc. Am. J., 6, 389–403, 1989.
Wessolek, G., Bohne, K., Duijnisveld, W., and Trinks, S.: Development of hydro-pedotransfer functions to predict capillary rise and actual evapotranspiration for grassland sites, J. Hydrol., 400, 429–437, 2011.
Weynants, M., Vereecken, H., and Javaux, M.: Revisiting Vereecken Pedotransfer Functions: Introducing a Closed-Form Hydraulic Model, Vadose Zone J., 8, 86–95, 2009.

HESSD
9, 3237–3267, 2012

Wigmosta, M. S., Vail, L., and Lettenmaier, D. P.: A distributed hydrology-vegetation model for complex terrain, Water Resour. Res., 30, 1665–1679, 1994.

Wosten, J. H. M.: Pedotransfer functions to evaluate soil quality, in: Soil quality for crop production and ecosystem health Development, edited by: Gregorich, E. G. and Carter, M. R., Soil Sci., 25, 221–245, 1997.

Xiao, Q., McPerson, E., Ustin, S., and Grismer, M.: A new approach to modelling tree rainfall interception, J. Geophys. Res., 105, 173–188, 2000.

HESSD

9, 3237–3267, 2012

Table 1. Soil properties for 26 FAO '74 main soils, including total soil depth and layering (d), sand (sa) silt (si) and clay (cl) content, permanent wilting point (θ_r), field capacity (θ_s), van Genuchten parameters (α, n), and hydraulic conductivity at saturation (k_s).

Soil	[cm]	[%]	[%]	[%]	[$cm^3\,cm^{-3}$]	[$cm^3\,cm^{-3}$]	[cm^{-1}]	[–]	[$cm\,d^{-1}$]
Acrisol	145								
1	13	58	23	19	0.058	0.389	0.024	1.369	18.9
2	20	54	21	25	0.068	0.395	0.023	1.340	11.9
3	28	48	20	32	0.076	0.406	0.023	1.301	7.6
4	41	43	19	37	0.082	0.419	0.023	1.280	7.1
5	43	44	20	36	0.081	0.416	0.023	1.287	6.8
Cambisol	134								
1	15	36	38	26	0.073	0.421	0.011	1.462	8.2
2	17	32	40	28	0.077	0.431	0.010	1.469	10.5
3	24	33	41	26	0.074	0.426	0.009	1.489	11.3
4	33	35	38	26	0.074	0.425	0.011	1.458	8.3
5	39	37	39	24	0.070	0.417	0.010	1.478	8.8
Chernozem	169								
1	31	16	52	31	0.086	0.458	0.008	1.514	12.6
2	26	16	53	31	0.085	0.461	0.008	1.516	12.2
3	24	16	54	30	0.084	0.458	0.007	1.528	12.2
4	35	17	55	28	0.081	0.452	0.007	1.550	12.3
5	53	20	54	26	0.078	0.443	0.006	1.566	12.7
Podzoluvisol	169								
1	19	40	50	10	0.045	0.405	0.007	1.590	33.3
2	14	40	52	8	0.041	0.410	0.007	1.603	44.5
3	35	40	44	16	0.056	0.401	0.008	1.538	15.6
4	54	43	38	20	0.062	0.406	0.011	1.477	9.2
5	47	49	34	18	0.058	0.398	0.015	1.436	13.6

HESSD
9, 3237–3267, 2012

Table 1. Continued.

Soil	[cm]	[%]	[%]	[%]	[$cm^3\,cm^{-3}$]	[$cm^3\,cm^{-3}$]	[cm^{-1}]	[–]	[$cm\,d^{-1}$]
Rendzina	32								
1	32	48	31	21	0.063	0.400	0.016	1.414	11.6
Ferralsol	165								
1	14	45	19	36	0.080	0.414	0.023	1.282	7.2
2	21	42	18	40	0.084	0.423	0.024	1.260	8.1
3	31	39	18	44	0.087	0.435	0.025	1.242	9.1
4	48	37	17	46	0.089	0.438	0.025	1.232	10.3
5	41	37	17	46	0.089	0.438	0.025	1.232	10.3
Gleysol	122								
1	16	39	32	28	0.076	0.421	0.014	1.400	5.84
2	25	38	29	32	0.080	0.426	0.016	1.358	5.18
3	35	34	31	35	0.083	0.435	0.015	1.362	5.76
4	46	38	27	35	0.082	0.427	0.018	1.334	5.06
Phaeozem	142								
1	22	31	40	29	0.078	0.434	0.010	1.463	10.6
2	20	29	36	35	0.085	0.446	0.013	1.396	8.2
3	25	25	33	42	0.090	0.460	0.015	1.334	9.0
4	31	24	34	42	0.091	0.463	0.014	1.339	9.5
5	44	30	35	35	0.084	0.444	0.013	1.389	7.6
Lithosol	10								
1	10	75	11	14	0.052	0.378	0.032	1.451	42.8
Fluvisol	128								
1	19	38	38	24	0.070	0.415	0.011	1.469	8.0
2	27	35	38	28	0.076	0.429	0.011	1.450	8.1
3	36	36	37	27	0.074	0.423	0.011	1.449	7.5
4	43	41	33	26	0.072	0.414	0.014	1.419	6.7

HESSD
9, 3237–3267, 2012

Table 1. Continued.

Soil	[cm]	[%]	[%]	[%]	[$cm^3\ cm^{-3}$]	[$cm^3\ cm^{-3}$]	[cm^{-1}]	[–]	[$cm\ d^{-1}$]
Kastanozem	122								
1	18	31	46	23	0.070	0.422	0.007	1.543	13.9
2	19	29	45	26	0.075	0.431	0.008	1.519	12.8
3	23	18	40	42	0.094	0.475	0.013	1.370	13.4
4	24	20	46	34	0.087	0.461	0.009	1.464	12.3
5	38	25	49	26	0.076	0.436	0.007	1.544	12.9
Luvisol	119								
1	16	74	14	12	0.048	0.381	0.034	1.456	48.0
2	23	70	12	18	0.057	0.378	0.030	1.372	26.3
3	25	62	11	27	0.068	0.383	0.027	1.294	13.3
4	45	54	12	34	0.076	0.396	0.027	1.260	11.3
Greyzem	179								
1	23	21	55	24	0.074	0.437	0.006	1.588	13.2
2	22	15	58	27	0.081	0.452	0.006	1.566	12.3
3	42	15	52	33	0.088	0.467	0.009	1.494	12.4
4	33	15	54	32	0.087	0.467	0.008	1.501	12.0
5	59	20	50	30	0.083	0.453	0.008	1.516	12.3
Nitosol	149								
1	14	40	26	35	0.081	0.426	0.019	1.326	5.2
2	19	33	22	45	0.089	0.446	0.021	1.259	8.7
3	27	28	21	51	0.093	0.462	0.022	1.233	14.5
4	39	28	19	53	0.094	0.464	0.023	1.218	14.8
5	50	27	19	54	0.094	0.467	0.023	1.216	15.4
Histosol	150								
1	20	42	21	38	0.083	0.424	0.022	1.282	6.4
2	23	28	38	35	0.085	0.451	0.012	1.408	9.6
3	37	31	30	40	0.087	0.447	0.016	1.326	6.8
4	40	54	24	22	0.064	0.394	0.022	1.366	14.0
5	30	74	13	14	0.051	0.381	0.033	1.435	40.7

HESSD
9, 3237–3267, 2012

Table 1. Continued.

Soil	[cm]	[%]	[%]	[%]	[$cm^3\ cm^{-3}$]	[$cm^3\ cm^{-3}$]	[cm^{-1}]	[–]	[$cm\ d^{-1}$]
Podzol	134								
1	14	77	16	7	0.041	0.385	0.040	1.564	72.8
2	17	79	16	5	0.038	0.387	0.042	1.655	91.1
3	16	80	15	6	0.040	0.387	0.042	1.667	91.5
4	27	81	13	6	0.042	0.384	0.040	1.726	102.8
5	50	85	11	4	0.043	0.384	0.040	2.033	168.0
Arenosol	170								
1	19	88	7	6	0.050	0.380	0.035	2.203	213.7
2	24	88	7	6	0.050	0.380	0.035	2.203	213.7
3	34	88	6	6	0.051	0.377	0.034	2.236	223.0
4	93	86	8	7	0.049	0.380	0.035	1.992	157.3
Regosol	87								
1	20	41	49	10	0.045	0.403	0.007	1.578	31.1
2	33	42	49	9	0.042	0.404	0.007	1.572	33.6
3	34	46	44	10	0.043	0.397	0.010	1.516	25.7
Solonetz	140								
1	12	52	28	20	0.061	0.395	0.019	1.394	14.6
2	17	47	26	27	0.072	0.406	0.019	1.363	8.4
3	24	42	26	32	0.078	0.417	0.018	1.342	5.8
4	35	39	29	33	0.080	0.427	0.017	1.356	5.2
5	52	42	28	30	0.077	0.416	0.017	1.365	6.1
Andosol	151								
1	23	50	36	14	0.050	0.392	0.014	1.451	18.6
2	25	55	32	12	0.046	0.387	0.019	1.421	27.1
3	29	56	33	12	0.045	0.391	0.020	1.420	27.9
4	30	55	32	13	0.048	0.389	0.019	1.419	25.1
5	42	59	28	13	0.047	0.387	0.024	1.400	28.3
Ranker	35								
1	16	52	25	18	0.057	0.394	0.018	1.409	16.3
2	19	57	24	19	0.058	0.390	0.023	1.374	18.4

HESSD
9, 3237–3267, 2012

Table 1. Continued.

Soil	[cm]	[%]	[%]	[%]	[$cm^3\ cm^{-3}$]	[$cm^3\ cm^{-3}$]	[cm^{-1}]	[–]	[$cm\ d^{-1}$]
Vertisol	127								
1	15	27	25	48	0.092	0.462	0.019	1.263	12.5
2	31	24	20	55	0.095	0.472	0.021	1.219	17.1
3	35	23	20	57	0.096	0.477	0.021	1.212	17.3
4	46	31	20	50	0.092	0.457	0.023	1.231	12.5
Planosol	103								
1	17	55	28	17	0.055	0.391	0.021	1.397	19.4
2	21	57	24	19	0.058	0.390	0.023	1.374	18.4
3	27	41	25	35	0.081	0.424	0.020	1.320	5.4
4	38	42	26	32	0.078	0.417	0.018	1.342	5.8
Xerosol	122								
1	17	34	45	21	0.066	0.414	0.007	1.543	14.5
2	25	33	42	25	0.072	0.424	0.009	1.501	12.1
3	38	31	43	26	0.074	0.428	0.009	1.504	12.4
4	42	36	41	23	0.069	0.416	0.009	1.500	10.9
Yermosol	131								
1	13	48	41	11	0.044	0.394	0.012	1.487	22.4
2	20	47	41	13	0.005	0.396	0.011	1.491	18.2
3	25	44	36	20	0.062	0.403	0.012	1.458	9.6
4	36	50	32	18	0.058	0.395	0.016	1.424	14.9
5	37	33	49	18	0.061	0.411	0.006	1.589	18.0
Solonchak	123								
1	8	41	23	37	0.083	0.425	0.021	1.298	5.7
2	17	45	18	37	0.081	0.414	0.024	1.272	7.7
3	23	27	35	39	0.088	0.457	0.014	1.362	8.6
4	21	33	32	36	0.084	0.441	0.015	1.361	6.2
5	54	35	27	39	0.086	0.439	0.018	1.313	5.5

HESSD
9, 3237–3267, 2012

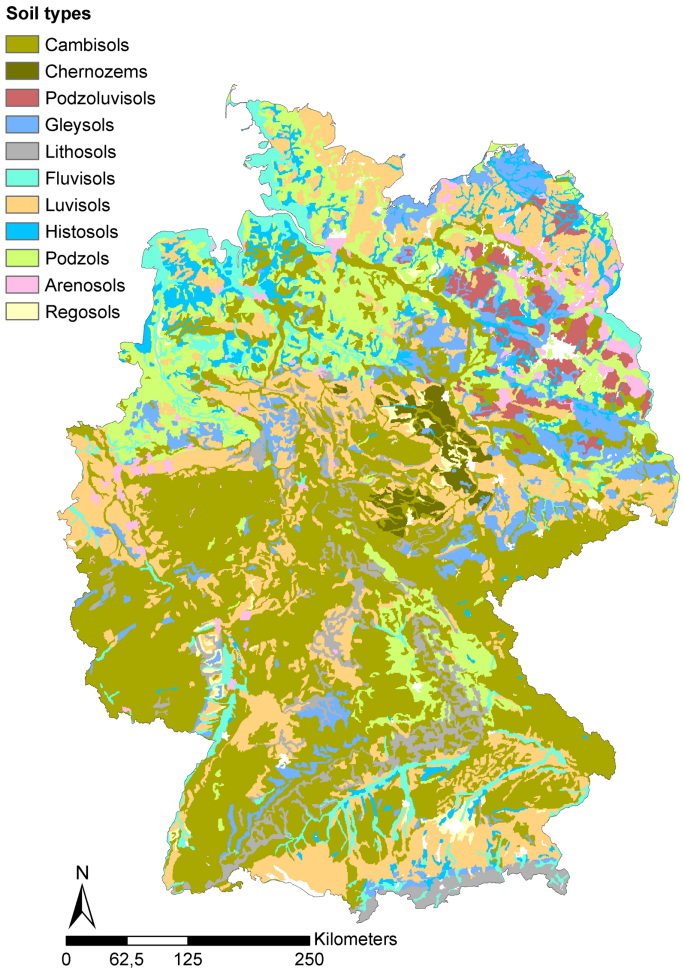

Fig. 1. Main soil types for Germany following the FAO '74 systematic (FAO, 1974).

HESSD
9, 3237–3267, 2012

A remote sensing based interception-infiltration model

M. Tum and E. Borg

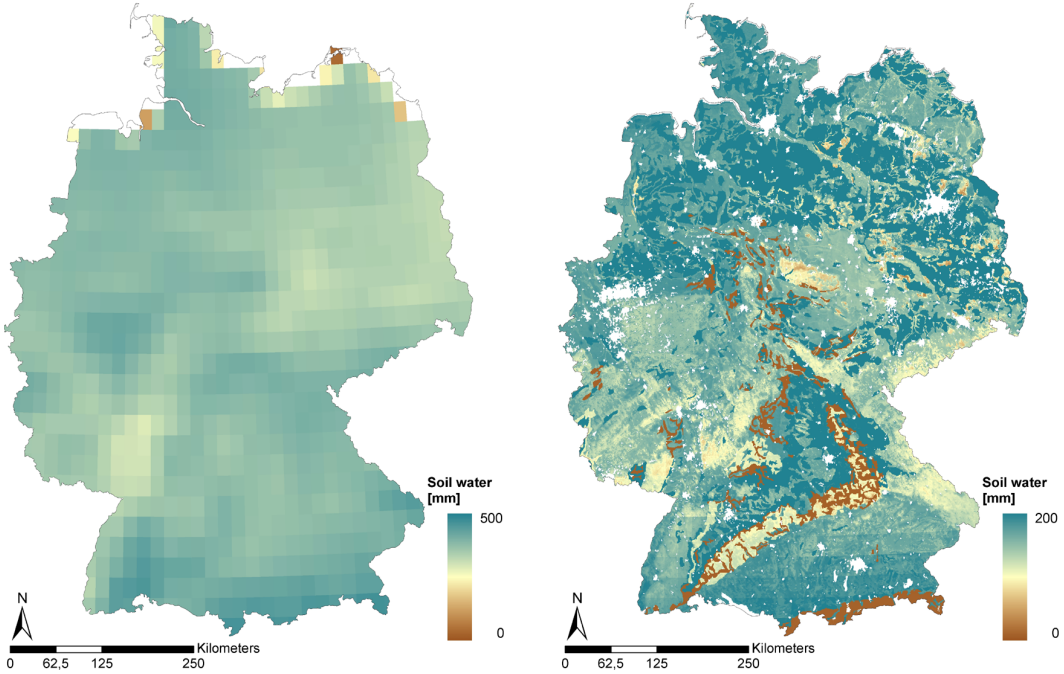

Fig. 2. Averaged plant available soil water content given in millimetres for the period 2002 to October 2007 for ECMWF (left panel) and own estimations (right panel). High values are shown in blue, moderate values in yellow and low values in red. Whit pixels represent no data.

HESSD
9, 3237–3267, 2012

A remote sensing based interception-infiltration model

M. Tum and E. Borg

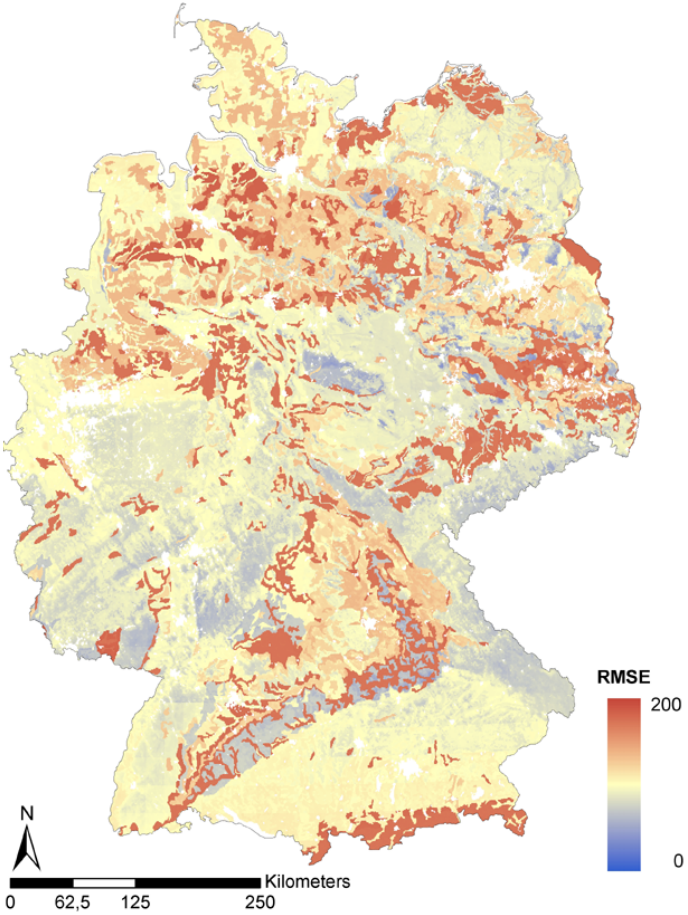

Fig. 3. Spatial distribution of RMSE for ECMWF simulation and our own time series simulation (2002 to October 2007) for Germany. Low RMSE are shown in blue, moderate in yellow and high in red. White pixels represent urban areas and water bodies.

HESSD
9, 3237–3267, 2012

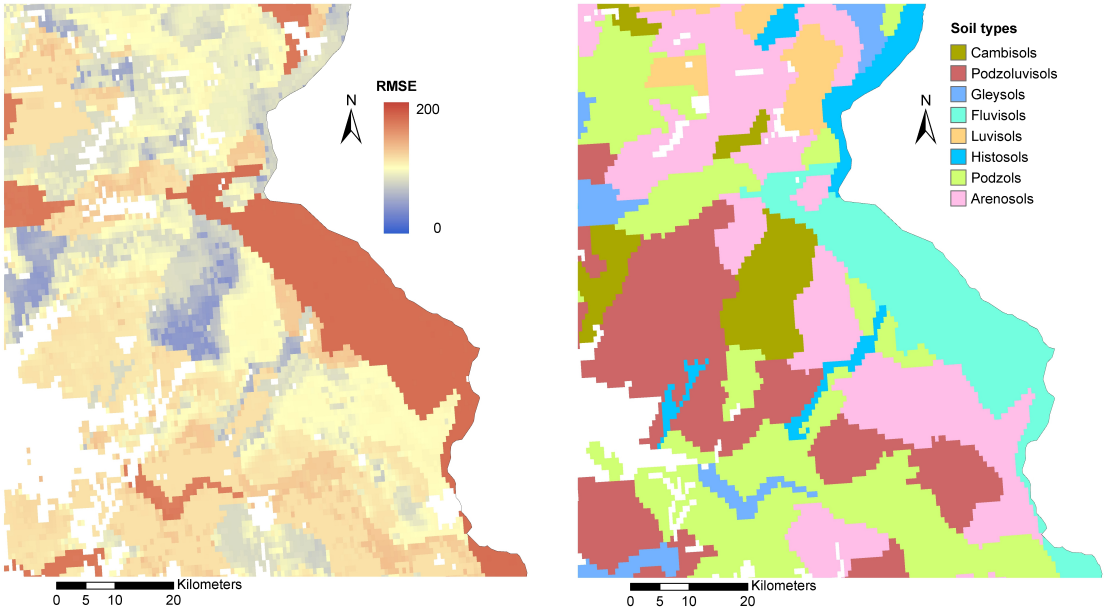

Fig. 4. RMSE (left panel) and main soil types (right panel) for the "Oderbruch-region" in East-Germany. The colour scheme follows the schemes of Fis. 1 and 3.

HESSD
9, 3237–3267, 2012

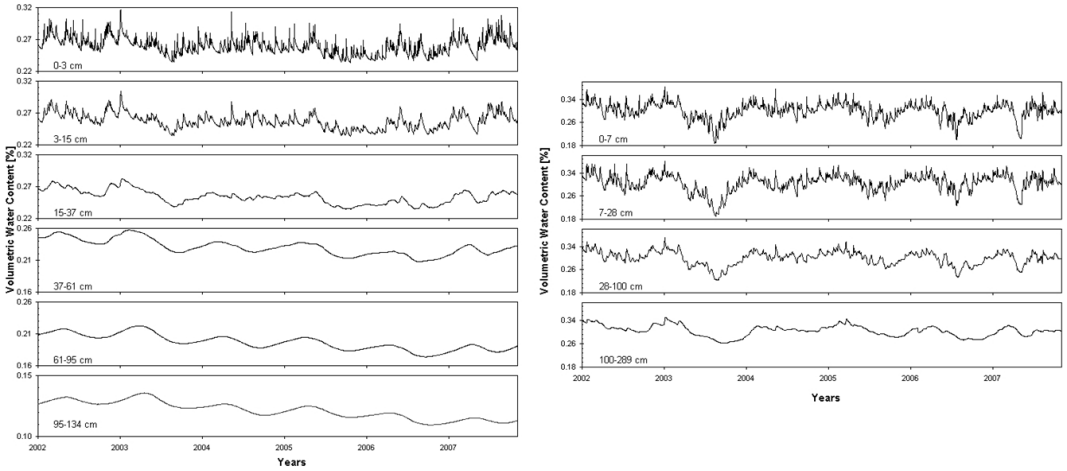

Fig. 5. Volumetric water content for a Cambisol site at 8.0° longitude/51.0° latitude. Left panel: own model results for six soil layers (0–3 cm, 3–15 cm, 15–37 cm, 37–61 cm, 61–95 cm, 95–134 cm). Right panel: ECMWF results for four soil layers (0–7 cm, 7–28 cm, 28–100 cm, 100–289 cm). Values are given per soil layer on a daily basis from January 2002 to October 2007.

HESSD
9, 3237–3267, 2012

A remote sensing based interception-infiltration model

M. Tum and E. Borg

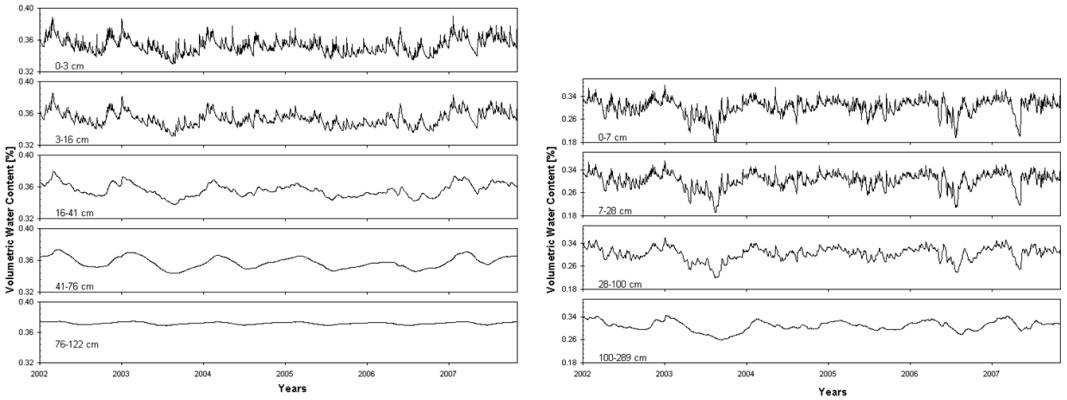

Fig. 6. Volumetric water content for a Gleysol site at 13.0° longitude/52.8° latitude. Left panel: own model results for five soil layers (0–3 cm, 3–16 cm, 16–41 cm, 41–76 cm, 76–122 cm). Right panel: ECMWF results for four soil layers (0–7 cm, 7–28 cm, 28–100 cm, 100–289 cm). Values are given per soil layer on a daily basis from January 2002 to October 2007.

HESSD
9, 3237–3267, 2012

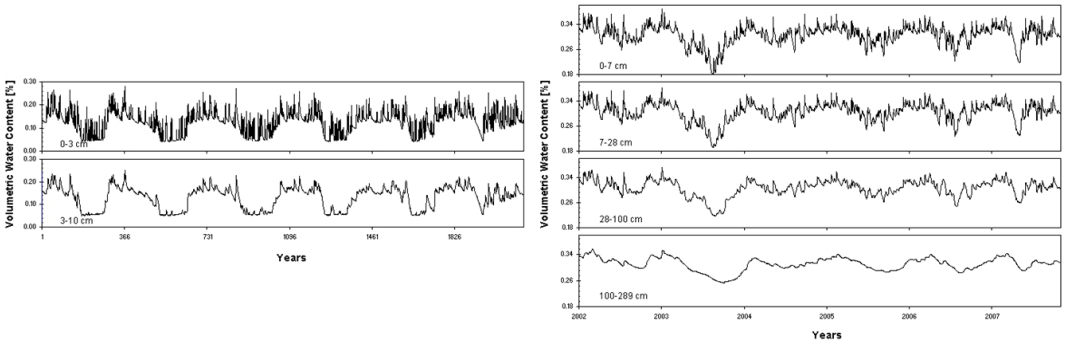

Fig. 7. Volumetric water content for a Lithosol site at 11.3° longitude/47.6° latitude. Left: own model results for two soil layers (0–3 cm, 3–10 cm). Right panel: ECMWF results for four soil layers (0–7 cm, 7–28 cm, 28–100 cm, 100–289 cm). Values are given per soil layer on a daily basis from January 2002 to October 2007.

HESSD
9, 3237–3267, 2012